Aerial Estimates of Methane and Carbon Dioxide Emission Rates Using a Mass Balance Approach in New York State

Alexandra M. Catena[1], Mackenzie L. Smith[2], Lee T. Murray[3], Eric M. Leibensperger[4], Jie Zhang[1], Margaret J. Schwab[1], James J. Schwab[1]

[1]Atmospheric Sciences Research Center, University at Albany, State University of New York, Albany, NY, USA

[2]Scientific Aviation, Inc. (Now Champion X), Boulder, CO, USA

[3]Department of Earth and Environmental Sciences, University of Rochester, Rochester, New York, USA

[4]Department of Physics and Astronomy, Ithaca College, Ithaca, NY, USA

Correspondence to: James J. Schwab (jschwab@albany.edu)

Abstract. Accurate greenhouse gas (GHG) emissions inventories are vital for climate mitigation as they can identify areas of need and ensure effective policy and regulation in reducing GHG emissions. Several studies have shown that self-reporting GHG inventories are undercounting methane emissions across all anthropogenic sectors showcasing an increasing need to validate the inventory with direct measurements. This study carried out aerial observations and emission rates of methane and carbon dioxide across multiple sectors in New York State (NYS). Emission rates were calculated for each of the sources using a mass balance method and were subsequently compared to the 2021 Environmental Protection Agency GHG Reporting Program (EPA GHGRP) Inventory. Landfills were the source of the highest observed methane emission estimates, ranging from 161–3440 kg/hr. There was also significant variation in observed emissions within facilities between seasons, indicating a significant influence from meteorology. Variation in estimated measured emissions between different landfills could be due to operational differences. Observed carbon dioxide emission estimates were dominated by combustion facilities followed by landfills. Comparisons with the inventory show that methane emissions averaged over ten observed landfills are underestimated by a factor of 2. However, out of the ten landfills, five landfills had observed methane emission estimates significantly higher than the inventory value, four landfills had an inventory value within the uncertainty range of the observations, and one landfill observed emission estimate was markedly lower than the reported inventory estimate. Seneca Meadows Landfill was the highest emitter from the measurements and was ~4.3x higher than the annual average estimate that was reported to the 2021 EPA GHGRP Inventory. NYS can use this information to inform the NYS GHG Inventory and improve emission estimation methodologies to better depict actual emissions.

1 Introduction

As a leading global greenhouse gas, methane (CH_4), and the reduction thereof, has presented itself as low hanging fruit in climate change mitigation. This is due to its warming potential of more than 80 times that of carbon dioxide (CO_2) over a 20-year timescale and its relatively short atmospheric lifetime of about a decade, as opposed to longer-lived CO_2, making its mitigation more cost-effective (Shindell et al., 2024; United Nations Environment Programme and Climate and Clean Air Coalition, 2021). There are several natural and anthropogenic sources of methane, with varying contributions to the global methane budget. In New York State (NYS), the largest anthropogenic sources include the fossil fuel, waste, and agriculture sectors, which accounted for 56%, 29%, and 15% of total state-wide anthropogenic methane emissions, respectively, according

to the 2021 NYS GHG Inventory (New York State Department of Environmental Conservation, 2023a). It is important to note that the NYS GHG Inventory and recently passed legislation use the 20-year global warming potential (GWP) metric while most national and international agencies use the 100-year GWP metric. Utilizing the 20-year GWP essentially emphasizes the higher warming impact of methane over 20 years as opposed to over 100 years due to methane's shorter atmospheric lifetime.

40   The 20-year GWP metric yields a much higher relative warming potential, which highlights the urgency in reducing methane over carbon dioxide emissions in the short-term.

There are some complexities that arise when trying to accurately assess the contributions from each of the sources of methane, which are primarily due to uncertainties in emission estimations. This uncertainty comes from inadequate measurements and

45   the inconsistent emission estimation results between top-down and bottom-up methods (Saunois et al., 2025). Top-down methods infer emissions through the use of chemical transport modeling and direct, in situ atmospheric measurements over regional- or global-scales to which they are scaled down to smaller facility- or process-level emissions (National Academies of Sciences, 2018). In contrast, bottom-up approaches are process-based methods, which estimate emissions based on activity data and emission factors (EF) from individual sources and are extrapolated to regional and national emission totals. These

50   activity data and EFs are a major source of uncertainty in bottom-up GHG inventories because they are not always representative of true emissions, but, given current understanding, are considered 'best estimates' (Miller and Michalak, 2017; Winiwarter and Rypdal, 2001). Several EFs for various sectors are based on data collected during studies from decades ago, which may not be indicative of current emissions (Lamb et al., 2016; National Academies of Sciences, 2018). In addition to that, since emission inventories are annual averages based on activity data and EFs, they do not account for seasonal or

55   operational changes between facilities, which have shown to result in significant differences in emissions seasonally and between facilities (Bell et al., 2017; Cusworth et al., 2021, 2024). However, inventories are developed with information available, and thus, lack of direct measurements of facilities to inform the inventories plays into the highly uncertain emission estimates, which is the case in NYS where there are few studies of methane observations from major sources of methane.

60   This high uncertainty in emissions inventories has led to a need for verification using top-down direct measurements. Numerous studies have shown that the reporting protocol used to comply with regulations for emissions inventories has resulted in an undercounting and underreporting of actual emissions across multiple sectors (Bergamaschi et al., 2015; Cusworth et al., 2024; Daniels et al., 2023; Foster et al., 2017; Guha et al., 2020; Lamb et al., 2016; Liu et al., 2023; Moore et al., 2023; Wecht et al., 2014; Yu et al., 2021). Top-down methods can evaluate emissions inventories by comparing these

65   inventories with a combination of direct measurements and chemical transport modeling. Top-down constraints afforded by aircraft or satellite observations have been critical in estimating and validating the emission rates of facilities or regions by their ability to sample the whole perimeter of the facility or regional area up to the planetary boundary layer height (Conley et al., 2017; Guha et al., 2020). A mass balance approach of a point source can estimate emissions from aircraft data by applying Gauss's Theorem to the reported methane enhancement and observed winds as the aircraft circles in a virtual cylinder around

the facility up to the boundary layer height (Conley et al., 2017; Cusworth et al., 2024; Koene et al., 2024). By sampling upwind and downwind of the facility, this allows full characterization of the facility-generated plume (Conley et al., 2017). These top-down estimations may then be compared to the values self-reported to the Environmental Protection Agency (EPA) Greenhouse Gas Reporting Program (GHGRP), which mandates large emitters of GHGs to report their emissions under 40 CFR Part 98 (CFR, 2009). The self-reporting GHGRP is separate from the NYS GHG Inventory in that it provides nation-wide facility-level emission totals while the NYS GHG Inventory only provides emission source totals across the state (e.g. all landfills or power plants). The NYS Inventory is used for regulatory purposes and allows for tracking and mitigating state-wide greenhouse gas emissions, while the GHGRP provides facility-specific information and allows for direct comparisons with observations. While it is difficult to make a rigorous comparison between limited observations and the annually averaged inventory, these limited observations help constrain our understanding of emissions from these facilities and highlight any areas of need for further investigation.

In 2019, NYS passed the Climate Leadership and Community Protection Act (CLCPA) that mandates a 40% reduction in GHG levels by 2030 and 85% reduction in GHG levels by 2050 as compared to 1990 levels (New York State Climate Action Council, 2022). In order to achieve these goals, the NYS GHG emissions inventory must be accurate since it is the basis for climate policy and regulation. To verify the accuracy of the inventory, aircraft measurements were carried out in NYS at combustion, landfill, wastewater treatment plant (WWTP), and agricultural facilities to compare against the self-reported GHGRP inventory. This paper reports the observed emission estimate results, which were calculated from a mass balance method using Gauss's Theorem across these source sectors. The aircraft emission estimates will be compared with the bottom-up EPA GHGRP Emissions Inventory. The results from this paper will help inform the inventory, improve our understanding in estimating accurate emissions, and help NYS meet the goals of the CLCPA.

2 Methods

The aircraft measurements were carried out over two separate field campaigns, which occurred in June and November/December 2021. With funding from the NYS Energy Research and Development Authority (NYSERDA), the main objective of the study was to determine emission rates from major methane sources in NYS to inform the NYS GHG Inventory. The focus of this study was primarily on methane emissions, but carbon dioxide was also measured as a co-pollutant and is reported in this manuscript. The aircraft measurements reported in this study were coordinated with a separate study done by Ravikumar et al. (2025), which focused on identifying and estimating methane emissions from natural gas transmission and storage compressor stations in NYS. This study focuses on aircraft sampling over waste incineration, industrial, power plant, waste, and agricultural facilities.

Table 1 lists the facilities sampled along with the facility name, type, date of sampling, number of laps made around each facility, minimum and maximum flight level, and mean radius of the loops. Figure 1 is a map illustrating all visited facilities for this study. The sites listed in the table were chosen by the project team, which balanced reported and estimated emission rates in the NYS GHG Inventory and their proximity to the airport bases in Rochester and Albany, NY.

105

The aerial measurements were completed by the Colorado-based scientific research company, Scientific Aviation, Inc. (now, Champion X), which used a Mooney single engine propeller aircraft. There were a total of 25 sites sampled from this study, with 5 sites visited more than once. Additional aircraft missions were flown in the vicinity of New York City, but due to flight restrictions of nearby airports, the aircraft could not sample extensively enough to present reliable fluxes from facilities within the New York City Area. Consistent with the Ravikumar et al. (2025) flights, all measurements were taken in the middle of the day from 10 am up to 5 pm local time to ensure the entirety of the emission plume was captured in a well-mixed and developed boundary layer.

Trace gases were measured by sampling ambient air drawn through rearward-facing inlets mounted on the wing of the aircraft. Observations of CH_4, CO_2, carbon monoxide (CO), and water vapor (H_2O) were recorded using a Picarro G2401 gas analyzer, which is a Wavelength-Scanned cavity ring-down spectrometer (https://www.picarro.com/environmental/g2401_analyzer_datasheet). The analyzer has a 1 σ precision of <1 parts per billion (ppb) of CH_4 and <50 ppb of CO_2 at 5 seconds. Calibrations were done inflight, along with measurements of temperature and relative humidity from a Vaisala HMP60 probe, and GPS coordinates from a Hemisphere high-precision differential GPS. Horizontal wind speed and direction were calculated following the method outlined in Conley et al. (2014). All 1 Hz data was interpolated. Further descriptions and discussion of the Scientific Aviation aircraft, analyzer precision and accuracy, and met data can be found elsewhere (Conley et al., 2017; Karion et al., 2015; Peischl et al., 2016; Ravikumar et al., 2025; Smith et al., 2015)

125 **Table 1: Information pertaining to all sites included in the analysis. The table provides the site name, location, sector, facility type, date of sampling, total number of laps completed around the facility, the lowest and highest altitudes above mean sea level (AMSL) reached at each facility, and the mean radius of the laps.**

Site	Sector	Facility Type	Date	Laps	Lowest Altitude AMSL (m)	Highest Altitude AMSL (m)	Mean Radius (m)
Covanta Niagara (43.085, -79.008)	Combustion	Waste Incinerator	6/15/2021	17	322	732	1137
Sithe Independence Station (43.494, -76.452)	Combustion	Power Plant	6/16/2021	16	227	851	1236

Sylvamo (43.891, -73.401)	Combustion	Waste, Pulp, and Paper	6/17/2021	12	179	694	1079
Globalfoundries US Inc Fab 8 (42.971, -73.754)	Combustion	Industrial	6/17/2021	7	227	473	911
Modern Landfill (43.212, -78.974)	Waste	Landfill	6/15/2021	16	247	634	1100
	Waste	Landfill	11/21/2021	16	247	514	1591
	Waste	Landfill	12/7/2021	10	246	595	1730
Seneca Meadows Landfill, Inc. (42.925, -76.846)	Waste	Landfill	6/16/2021	16	292	906	1695
	Waste	Landfill	11/17/2021	16	291	608	2560
	Waste	Landfill	12/7/2021	12	295	794	1947
Ontario County Landfill (42.854, -77.081)	Waste	Landfill	6/16/2021	13	404	946	1305
	Waste	Landfill	11/17/2021	13	397	596	1618
High Acres Landfill (43.083, -77.373)	Waste	Landfill	6/16/2021	19	292	1170	1484
	Waste	Landfill	11/19/2021	3	336	475	1388
	Waste	Landfill	11/21/2021	14	292	556	1876
Riga Mill Seat Landfill (43.056, -77.934)	Waste	Landfill	6/15/2021	10	347	557	1025
	Waste	Landfill	11/21/2021	15	359	575	1718
DANC SWMF (43.82, -75.917)	Waste	Landfill	6/17/2021	13	447	925	1341
Albany Landfill (42.71, -73.851)	Waste	Landfill	6/17/2021	11	234	619	942
Hyland Landfill (42.284, -78.011)	Waste	Landfill	6/15/2021	12	664	1171	1117
Chafee Landfill (42.581, -78.502)	Waste	Landfill	6/15/2021	13	584	826	995
Ava Landfill (43.456, -75.415)	Waste	Landfill	6/17/2021	18	565	1247	1154
Bird Island STP (42.924, -78.901)	Waste	WWTP	6/15/2021	9	326	679	1103
Frank E Van Lare STP (43.237, -77.577)	Waste	WWTP	6/16/2021	15	230	755	775
Onondaga Metro Syracuse STP (43.064, -76.172)	Waste	WWTP	6/16/2021	13	288	763	1358
ACSD North STP (42.676, -73.727)	Waste	WWTP	6/17/2021	11	152	590	637
Farm #1	Agriculture	CAFO	6/15/2021	12	360	789	892
Farm #2	Agriculture	CAFO	6/15/2021	8	316	478	797
Farm #3	Agriculture	CAFO	6/16/2021	15	270	706	837

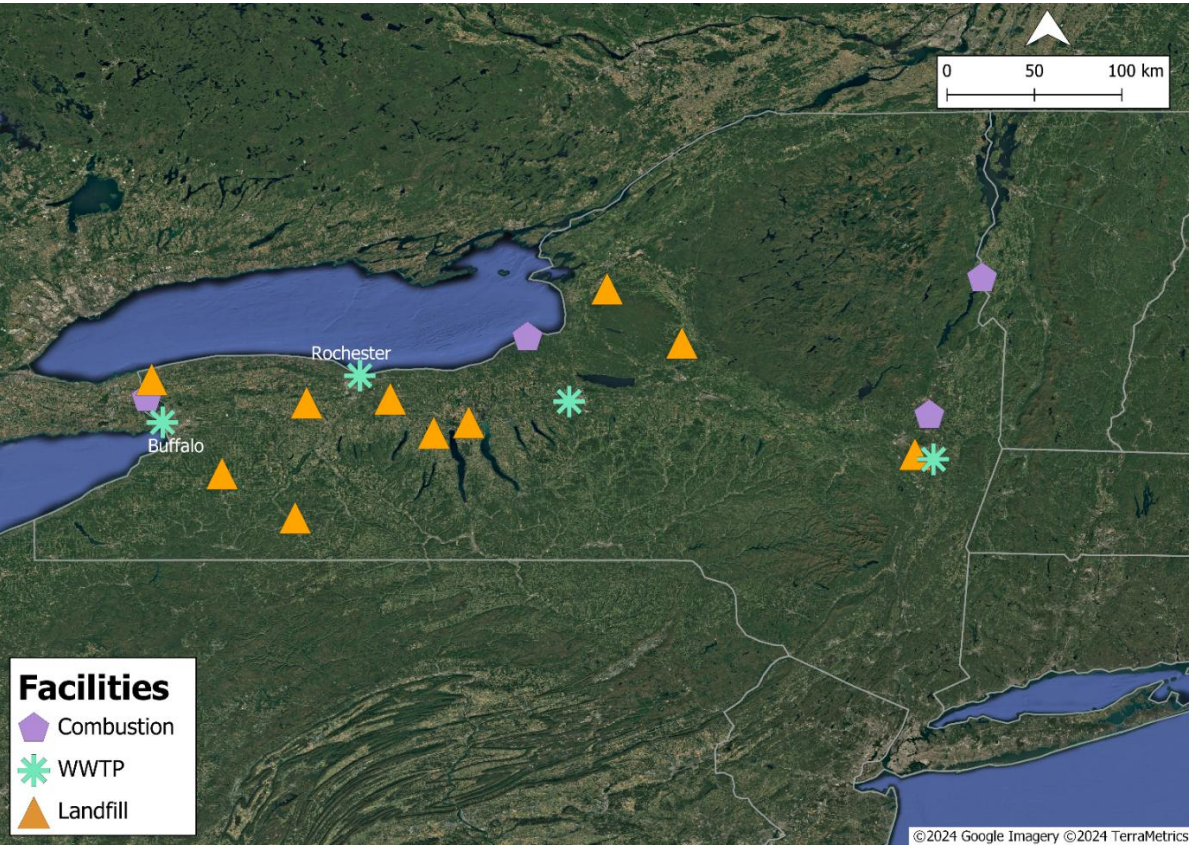|							
Farm #4	Agriculture	CAFO	6/16/2021	13	281	682	696
Farm #5	Agriculture	CAFO	6/17/2021	15	376	950	1024
Farm #6	Agriculture	CAFO	11/17/2021	11	430	605	1989
Farm #7	Agriculture	CAFO	11/17/2021	14	402	599	1972

Figure 1: Map of all sites sampled in the study, which include combustion facilities, landfills, wastewater treatment plants (WWTP), and industrial sites. Locations of the concentrated animal feeding operations (CAFO) sampled are not identified following United States federal privacy laws. Combustion facilities include a waste incinerator plant, power plant, industrial facility, and a waste, paper, and pulp facility. This map was created in QGIS (https://qgis.org/) using Google Satellite Imagery, accessed on 19 August 2024.

2.1 Mass Balance Emission Estimation

Emission estimates for each sampled facility were calculated from a mass balance method using Gauss's Theorem (Conley et al., 2017; Ravikumar et al., 2025). As the aircraft flies in a spiral pattern defining a virtual cylinder above the facility, the total

6

140 flux contribution from the facility is estimated from the product of the methane observations with the horizontal wind flow and summed over each height level. The total contribution from the facility is estimated by integrating the outward horizontal flux at each point along the flight path. This is done by following the mass balance equation below (Conley et al., 2017):

$$Q_c = \left\langle \frac{\partial m}{\partial t} \right\rangle + \int_0^{z_{max}} \oint c' \boldsymbol{u_h} \cdot \hat{n} \, dl \, dz, \tag{1}$$

145

where Q_c is the emission rate, z_{max} is the top of the sampling height, c' is the deviation from the mean concentration for each loop, such that $C = \bar{c} + c'$, where C is the measured concentration and $\bar{c}$ is the mean concentration per loop, $\boldsymbol{u_h}$ is the horizontal wind vector, $\hat{n}$ is the outward pointing unit vector, dl is the change in length per sample, and dz is the change in height between each loop around the facility. The volume mixing ratio is converted to a mass mixing ratio using the ideal gas law, and then

150 multiped by the altitude-dependent density to obtain mass concentration. The storage term, $\left\langle \frac{\partial m}{\partial t} \right\rangle$, is calculated as the time rate of change of the average mass concentration within the sampled volume throughout the entire period of measurements. Numerically integrating Eq. (1) yields Eq. (2) (Conley et al., 2017):

$$Q_c = \frac{\Delta m}{\Delta t} + \sum_{z=0}^{z=Z_{max}} \left(\sum_0^L \left(\rho \cdot c' \cdot \frac{MW_{CH_4}}{MW_{AIR}} \cdot u_n \right) \cdot \Delta s \right) \cdot \Delta z \tag{2}$$

155

The second term in Eq. (2), the net outflow term, estimates the contribution from the facility by summing the product of the scalar air density (ρ) as a function of height, the wind speed normal to the flight path (u_n), the fraction of the molecular weight of methane to air $\left(\frac{MW_{CH_4}}{MW_{AIR}} \right)$, and change in distance between each time step over the distance of one entire loop (L). This calculates a total product sum for each loop. The loops are then aggregated into 6 equal height bins from the lowest ($z = 0$) to

160 the highest flight level ($z = Z_{max}$). The lowest layer extended from the lowest measured flight altitude to the surface, which varied from site to site. For loops within the same height bin, the total product sum from those loops were averaged. The total product sum was then multiplied by the height bin width (Δz) and then summed over each height bin.

The remaining term in Eq. (2) is the storage term, which is estimated using the time rate of change of the average mass

165 concentration from loop to loop over the full flight. The area is determined by applying the Convex Hull function in Python to the measured x and y coordinates, which is then multiplied by the maximum measured altitude above ground level to estimate the total volume. The rate of change, or slope, is determined from the average mass concentration from each loop with time in [kg m^{-3} s^{-1}] and is then multiplied by the volume of the sampled area to get the rate of change of the mass concentration over the entire period of measurements at the given facility. This total rate of change or storage term is then added to the net outflow

170 term from Eq. (2) to get the net total emission rate (Q_c) of the facility. Typical average values of the dl and dz terms are ~70 m and ~72 m, respectively. The spiral pattern of the aircraft led to an average of ±17 m variation in height within each loop.

The Conley et al. (2017) study assumed a near zero vertical mixing at the top of the plume, which was proved to be an accurate assumption as shown in the first figure of their paper. Figure 2 below depicts a typical flight pattern from this study and the measured methane mixing ratio profile at Seneca Landfill on 16 June 2021. Since the methane mixing ratio reduced to background levels at the highest flight level above the plume, the assumption from Conley et al. (2017) held true for this study as well.
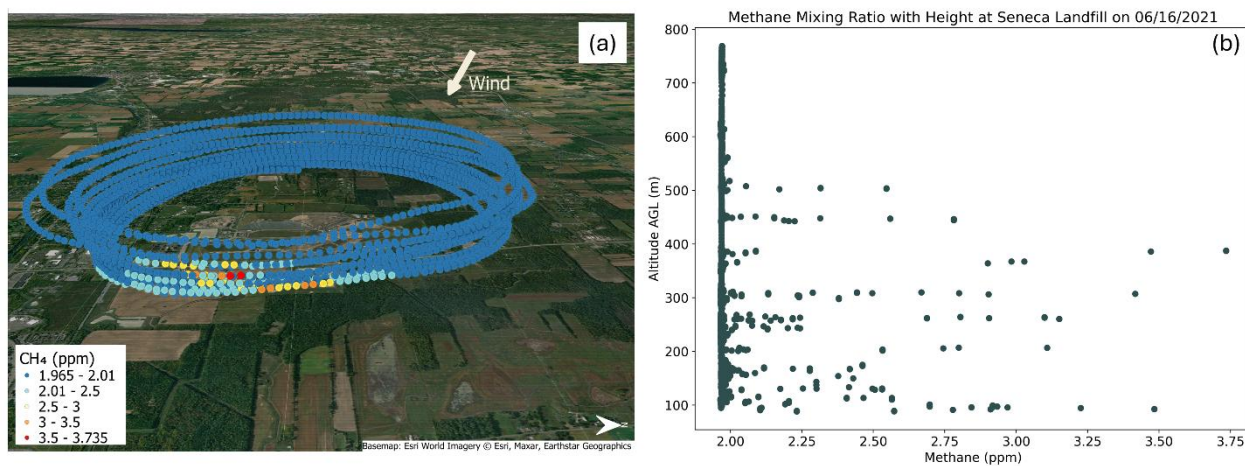

Figure 2: Panel (a) on the left depicts the flight path around Seneca Landfill on 06/16/2021. Methane mixing ratios in parts per million (ppm) were measured at multiple altitudes with varying concentrations. Panel (b) on the right is a profile of the observed methane plume.

2.2 Sources of Uncertainty

There are several sources of uncertainty with the mass balance approach using Gauss's Theorem including measurement error, wind parameterization from a moving aircraft, convective boundary layer height determination, interpolation of data, and pinpointing exact sources of interest without the interference of additional sources nearby (Cambaliza et al., 2014). Another major source of uncertainty in this method is the section of the plume that is not accounted for from the ground-level up to the lowest flight level (Cambaliza et al., 2014; Gordon et al., 2015). Assuming a well-mixed boundary layer, the methane mixing ratio is assumed to be constant from the surface up to the lowest flight level. Conley et al. (2017) analyzed several distances to the point source to determine the most ideal sampling distance. This consisted of determining a balance between being far enough from the source to ensure the near-surface plume has mixed well enough into the boundary layer with limited variability but close enough where there is discernable difference between the plume and background. This sampling distance method was done for this study using a combination of the convective boundary layer height, standard deviation of the wind speed, and a parameterization for the convective velocity scale, as done so in Conley et al. (2017). There is also the issue of additional

unintended sources included in the analysis in urban areas due to a higher number of adjacent sources, making it difficult to focus on one specific facility. Error could arise from either an additional source nearby or from the inability to sample the complete background concentration upwind. Another challenge with these direct measurements is the lack thereof. These observations were only a few days out of the year, which can lead to bias as they do not account for seasonal or operational changes and may not be representative of an annual emission rate. At the same time, these are the only observations available for these facilities, and they help bridge the data gaps of more reliable observations. These measurements were also performed during the daytime, which precludes consideration of any diurnal variation. This can also lead to error as previous studies have shown measurable diurnal variation in concentrations due to pressure changes, temperature, wind shear, and varying convective layer heights, especially from landfills (Delkash et al., 2022; Xu et al., 2014). However, the intensity of diurnal variation influences is mostly dependent on landfill management, such as methane generation rate, cover types of the landfill, gas collection, and climate (Delkash et al., 2022).

Uncertainties are estimated following the method outlined in Erland et al., 2022, which accounts for measurement error, the variability in the flux between height levels, and how stationary the plume is (Conley et al., 2017; Erland et al., 2022). The standard deviations between the heights are summed in quadrature to get the total uncertainty. The error in extrapolating to the surface is accounted for when estimating error from flux variation and is estimated as twice that of the error estimated for the lowest height bin (Erland et al., 2022). Referring to Table 2, Table 3, and Table 4 which lists the observed emission rates and their uncertainties for all sectors, the combustion facilities had a methane emission uncertainty average of about 48%, ranging from 18%–82%. Landfills were ~30%, ranging from 10%–80%. WWTPs showed much higher variation in uncertainty, ranging from 34%–1330%. Uncertainty for concentrated animal feeding operations (CAFO) averaged at about 60%, ranging from 32% up to 111%, not including one farm, which had an uncertainty of ~300%. These uncertainties are an estimate of the variation of the flux between each of the loops around a particular site only, which mostly takes into account the turbulent effects on the plume. It does not include any other potential source of uncertainty, including day-to-day or seasonal differences.

3 Results

3.1 Emission Rate Comparisons

The calculated emission rates from the aircraft observations and Eqs. (1) and (2) for the combustion, landfill and WWTP, and agricultural sources can be seen in Tables 2, 3, and 4, respectively. Observed emission rates were calculated for CH_4 and CO_2 for each of the facilities. Tables 2 and 3 also list the available self-reported 2021 EPA CH_4 and CO_2 GHGRP Inventory estimates. The EPA GHGRP methane estimates are converted from carbon dioxide equivalent using the 100-year GWP values from the Intergovernmental Panel on Climate Change (IPCC) Fourth Assessment Report (IPCC, 2007; Greenhouse Gas Reporting Program (GHGRP) [FLIGHT], 2022). The only facilities as part of this study required to report methane emissions to the EPA GHGRP are the landfills and combustion facilities, hence no available comparisons between the observations and

self-reported inventory values for the WWTP and CAFO facilities. Comparisons with the GHGRP are discussed in Section 3.2.

230

Observed methane emission rates varied widely both between and within the combustion, landfill, WWTP, and agricultural sectors. As seen in the comparison plots in Fig. 3, landfills were responsible for the highest observed methane emission rates ranging from 161–3440 kg h^{-1}, with an average of 1240 kg h^{-1}. The large range in values between the facilities can be due to several factors including operational differences, size of landfill, or waste quantity. Seneca Meadows Landfill accounted for

235   the largest observed methane emission estimate, which is consistent with its status as the largest landfill in New York State in terms of both current size and annual permits (New York State Department of Environmental Conservation, 2020).

There was also a large range in values within the facilities that were sampled more than once, and every one of the facilities exhibited higher emission estimates in the winter months compared to the summer months except for High Acres Landfill,

240   which showed the opposite. Between the summer and winter months, there was approximately a 45% difference at Modern, 42% difference at Ontario, 85% difference at High Acres, and 52% difference at Riga Mill Seat Landfill in methane emission estimates. Seneca Meadows Landfill was the only facility with relatively consistent emission rates, showing a ~15% difference between the summer and winter months. Variation in meteorological and environmental conditions, such as ambient pressure and temperature, wind, and soil moisture and temperature of the landfill have shown to impact methane emissions from

245   landfills, which can explain the seasonal differences in observed emission rates at these landfill facilities (Delkash et al., 2016, 2022; Poulsen et al., 2003; Rachor et al., 2013; Xu et al., 2014; Zhang et al., 2013). While these studies have shown seasonal influences on methane emissions, the results here only provide one day each from each season, which may leave out other possible influences like synoptic scale disturbances or operational differences.

250   There were several facilities that exhibited non-detectable or non-quantifiable observed emission rates, which can be due to several reasons, including inability to detect an upwind background and downwind enhancement, inability to quantify a plume within variable winds, or the facility location within an urban area with adjacent sources nearby. WWTPs showed mostly lower emission rates than landfills, ranging from 12.8–21.6 kg h^{-1}. Out of the five WWTP sampling days, three samples had non-detectable fluxes, likely due to the fact that they were located in urban areas and the aircraft was unable to get close enough to

255   the ground to sample the plume from the urban background. CAFOs and the combustion facilities exhibited a comparable range of methane estimates between each other from 3.5–182.8 kg h^{-1} and 6.7–118 kg h^{-1}, respectively. The large variation in the CAFOs could be due to a number of reasons. The CAFOs had different types of herds (i.e., dairy cows, swine, sheep and chickens), which would result in varying emissions (EPA, 2024). Although the largest farms were sampled, the exact herd size enclosed within the flight loops during sampling was not known since a particular farm could have several locations and the

260   central operating location given in the database does not always mean the herd is at that location. Lastly, manure management is a large source of methane within the livestock sector and is usually stored in lagoons away from the barns or central operating

locations, which could potentially leave it out of the area sampled by the aircraft and ultimately exclude it from the emission rate estimate.

265 As expected, the Sithe Independence natural gas power plant and Covanta Niagara waste incineration facility had by far the largest observed CO_2 emissions with a maximum emission rate of 300,000 kg h^{-1} and 129,783 kg h^{-1}, respectively, but emissions from landfills were still quite substantial and larger than the remaining sources with a maximum emission rate of 58,941 kg h^{-1}, which can be seen in Fig. 4.

270 **Table 2. Observed methane (CH_4) and carbon dioxide (CO_2) emission rates and their uncertainties from the waste incineration, power plant, industrial, and waste, paper, and pulp sector facilities in comparison to the available 2021 Environmental Protection Agency Greenhouse Gas Reporting Program (EPA GHGRP) Inventory value.**

Site	Facility Type	Date	Observed CH_4 Emission (kg h^{-1})	2021 EPA GHGRP CH_4 Emission (kg h^{-1})	Observed CO_2 Emission (kg h^{-1})	2021 EPA GHGRP CO_2 Emission (kg h^{-1})
Covanta Niagara	Waste Incinerator	6/15/2021	28.6 ± 7.3	29	129783 ± 68932	-
Sithe Independence Station	Power Plant	6/16/2021	118.2 ± 21.7	2.9	300003 ± 68951	157181
Globalfoundries US Inc Fab 8	Industrial	6/17/2021	n.d.*	0.05	338 ± 3091	2888
Sylvamo	Waste, Paper, and Pulp	6/17/2021	6.7 ± 4.5	226	32317 ± 11877	18402

*n.d. – not detected

275

Table 3. Observed methane (CH_4) and carbon dioxide (CO_2) emission rates and their uncertainties from the landfill and wastewater treatment plant sector facilities in comparison to the available 2021 Environmental Protection Agency Greenhouse Gas Reporting Program (EPA GHGRP) Inventory value.

Site	Facility Type	Date	Observed CH_4 Emission (kg h^{-1})	2021 EPA GHGRP CH_4 Emission (kg h^{-1})	Observed CO_2 Emission (kg h^{-1})	2021 EPA GHGRP CO_2 Emission (kg h^{-1})
Modern	Landfill	6/15/2021	785 ± 246	1343	1385 ± 4173	8.4

Riga Mill Seat	Landfill	6/15/2021	902 ± 295	673	7072 ± 2717	203
Hyland	Landfill	6/15/2021	484 ± 187	356	n.d.*	1.8
Chafee	Landfill	6/15/2021	890 ± 260	231	8180 ± 1850	168
Bird Island STP	WWTP	6/15/2021	n.d.	-	2245 ± 2421	-
Seneca Meadows	Landfill	6/16/2021	2789 ± 815	726	33233 ± 9448	2.1
Ontario County	Landfill	6/16/2021	983 ± 306	434	12240 ± 5030	12.4
High Acres	Landfill	6/16/2021	1346 ± 321	844	21967 ± 6064	164
Frank E Van Lare STP	WWTP	6/16/2021	13 ± 5	-	n.d.	-
Onondaga Metro Syracuse STP	WWTP	6/16/2021	n.d.	-	3013 ± 7869	-
DANC SWMF	Landfill	6/17/2021	456 ± 118	257	n.d.	10.2
Albany	Landfill	6/17/2021	161 ± 55	270	7254 ± 2379	-
Ava	Landfill	6/17/2021	323 ± 123	328	5873 ± 3160	10.3
ACSD North STP	WWTP	6/17/2021	22 ± 7	-	3835 ± 989	18402
Seneca Meadows	Landfill	11/17/2021	3099 ± 708	726	43546 ± 7144	2888
Ontario County	Landfill	11/17/2021	1507 ± 156	434	18381 ± 3172	2.1
High Acres	Landfill	11/19/2021	593 ± 490	844	5789 ± 10308	12.4
Modern	Landfill	11/21/2021	1277 ± 342	1343	n.d.	164
High Acres	Landfill	11/21/2021	488 ± 141	844	28882 ± 7374	8.4
Frank E Van Lare STP	WWTP	11/21/2021	n.d.	-	n.d.	164
Riga Mill Seat	Landfill	11/21/2021	1536 ± 564	673	12417 ± 5348	203
Modern	Landfill	12/7/2021	1260 ± 348	1343	14371 ± 4087	8.4
Seneca Meadows	Landfill	12/7/2021	3440 ± 803	726	58941 ± 21504	2.1

280 *n.d. – not detected

Table 4. Estimated emission rates from the agricultural sector facilities for methane (CH$_4$) and carbon dioxide (CO$_2$) and their uncertainties. The Environmental Protection Agency Greenhouse Gas Reporting Program (EPA GHGRP) Inventory is not available for CAFOs

Site	Facility Type	Herd Type	Date	Observed CH$_4$ Emission (kg h^{-1})	Observed CO$_2$ Emission (kg h^{-1})
Farm #1	CAFO	Dairy Cow	6/15/2021	53 ± 27	n.d.*
Farm #2	CAFO	Sheep	6/15/2021	8.5 ± 6.2	838 ± 605
Farm #3	CAFO	Chicken	6/16/2021	3.5 ± 3.9	n.d.
Farm #4	CAFO	Swine	6/16/2021	8.6 ± 3.5	n.d.
Farm #5	CAFO	Dairy Cow	6/17/2021	183 ± 59	5103 ± 3473
Farm #6	CAFO	Dairy Cow	11/17/2021	108 ± 68	n.d.
Farm #7	CAFO	Dairy Cow	11/17/2021	7.7 ± 24	n.d.

*n. d. – not detected
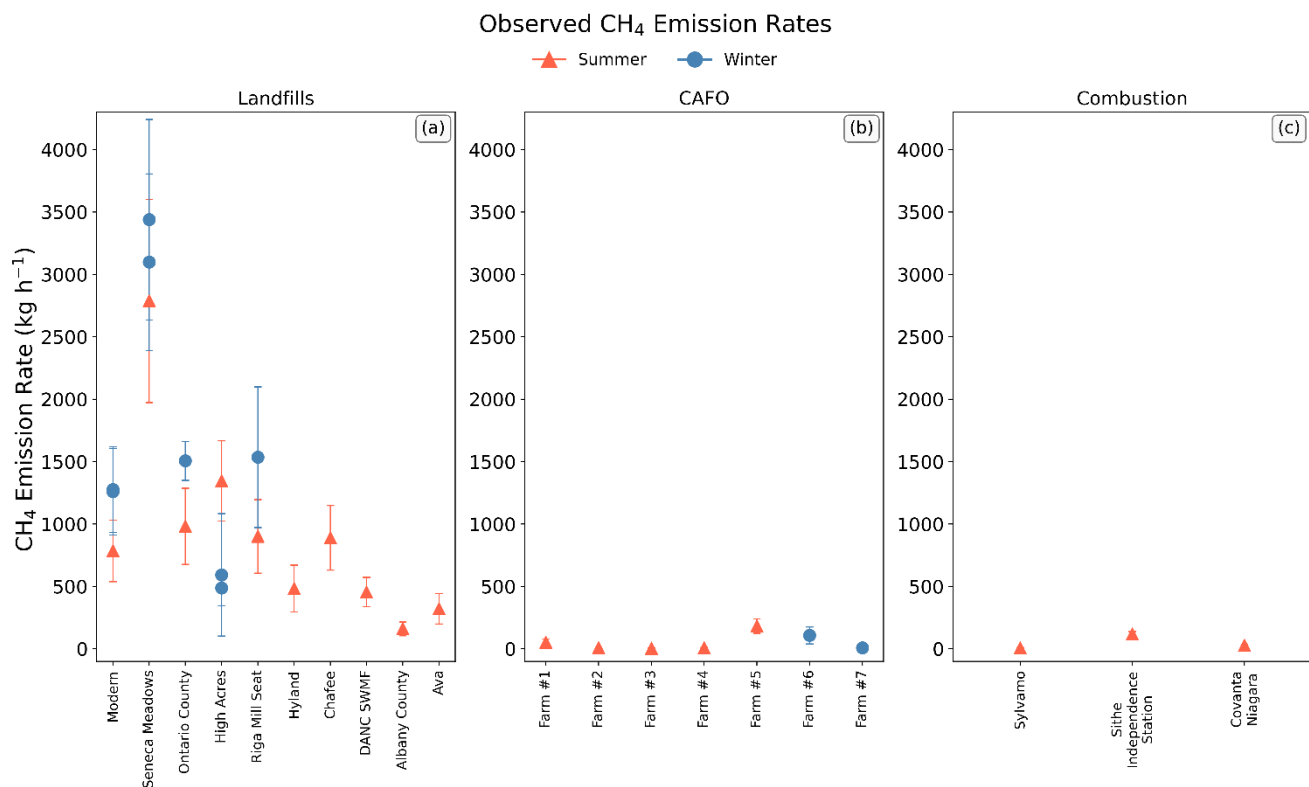
Figure 3: Observed methane (CH₄) emission rate comparisons between each of the sectors for (a) landfills, (b) concentrated animal feeding operations (CAFO), and (c) combustion facilities. The wastewater treatment plant observed emission rates were not included due to unreliable and low emissions.
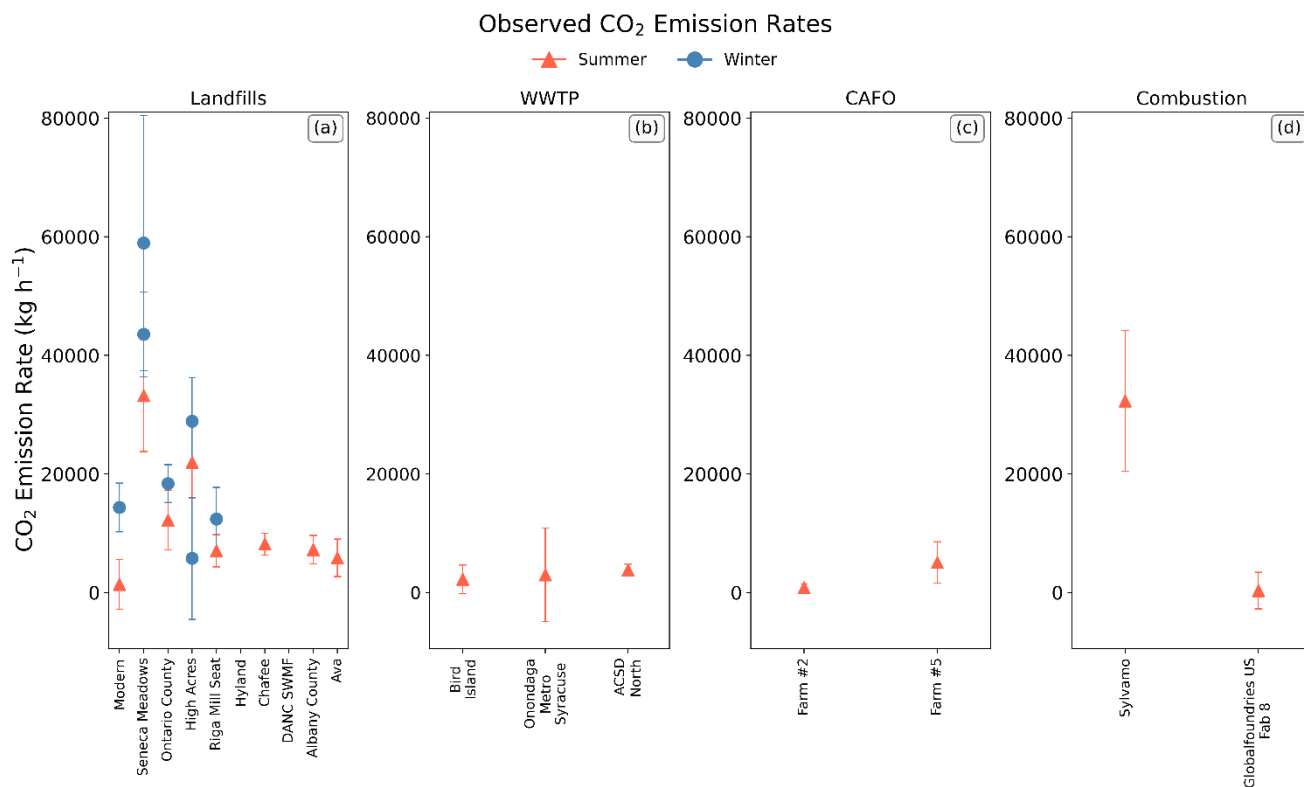
290

295

Figure 4: Observed carbon dioxide (CO₂) emission rate comparisons between each of the sectors for (a) landfills, (b) wastewater treatment plants (WWTP), (c) concentrated animal feeding operations (CAFO), and (d) combustion sources. The power plant and waste incinerator facilities were not included in this plot due to the significantly higher emission estimates.

3.2 2021 EPA GHGRP CH₄ Emission Inventory Comparisons

The methane emission estimates from this study have been compared to available methane emission rates self-reported to the EPA GHGRP (Greenhouse Gas Reporting Program (GHGRP) [FLIGHT], 2022). As mentioned previously, facility-level methane emission rates are not available under the 2021 NYS GHG Inventory (New York State Department of Environmental Conservation, 2023b). The comparisons between the methane observations from this study and the self-reported EPA GHGRP Inventory can be seen in Table 2, Table 3, and Fig. 5. As seen in Table 3, the observed landfill emission estimates were, on average, 2x greater than what was reported in the inventory. The highest observed emission rates were estimated from Seneca Meadows Landfill ranging from 2789–3440 kg h^{-1}, which were ~4.3x greater than the GHGRP self-reported value of 726 kg h^{-1}. Modern Landfill self-reported as the highest in-state point source emitter of methane at 1343 kg h^{-1}, yet the average observed estimate from the facility (~1107 kg h^{-1}) was lower than the inventory estimate. Nonetheless, the inventory estimate is still within the uncertainty range of the observed estimate rate at Modern, which is the case for three other landfills as well, including High Acres, Hyland, and Ava Landfill. Albany Landfill was the only landfill where the observed CH₄ emission rate

15

was relatively lower than the self-reported inventory value, at about 60% of the self-reported value. The remaining five landfills
315 all exhibited higher observed CH_4 emission estimates than what was reported in the inventory averaging at ~3.1x greater, including Seneca Meadows Landfill, Ontario County Landfill, Riga Mill Seat Landfill, Chafee Landfill, and Development Authority of the North Country (DANC) Solid Waste Management Facility. As seen in Fig. 5b, the methane emission rates varied widely between the combustion facilities for both the observed and the inventory estimates. The differences were also inconsistent– the Sylvamo Paper Mill mass balance estimate was ~34x lower than the inventory while the Sithe Independence
320 mass balance estimate was ~41x greater than the inventory. Figure 5 also shows the significantly higher methane emission rates from landfills over the combustion facilities. As seen in Table 3, the CO_2 emission rate comparisons between the observed and self-reported GHGRP values are significantly different at the landfill facilities due to EPA not accounting for biogenic CO_2 emissions. The inventory only accounts for combustion-related emissions of CO_2.

325 These results suggest that the self-reporting of methane emissions from landfills in NYS may be underestimated. However, there are a few cases where the GHGRP values are higher than the observations suggest. This inconsistent comparison with the inventory likely results from the assumptions employed by each landfill operator about the methane captured (all the landfills sampled employ methane capture technologies). Additionally, the discrepancies between the observed and reported values seen here echo what has been reported from previous studies, which is mostly due to differences in estimating the
330 emission rate between top-down and bottom-up approaches (Saunois et al., 2025). While this could explain the disagreement seen here between the observations and reported values, the mostly higher observations from this study follow a similar trend seen in other recent studies, which suggest that the methods followed in the inventory may not be accounting for all emissions (Bergamaschi et al., 2015; Cusworth et al., 2024; Daniels et al., 2023; Foster et al., 2017; Guha et al., 2020; Lamb et al., 2016; Liu et al., 2023; Moore et al., 2023; Wecht et al., 2014; Yu et al., 2021). However, there is some issue with trying to compare
335 the two when they may not be direct comparisons. The self-reported values are based on annual numbers, which can lead to uncertainties and inaccuracies in emissions inventories due to the effort of trying to consolidate the emission estimate into a single annual average rate and thus not accounting for seasonal and operational differences. On the contrary, individual observed emission rates may not be a direct comparison to the inventory estimates, since they are a snapshot from a few days of the year, as compared to the annual average from the inventory and may not be representative of typical emissions. At the
340 same time, these limited observations provide valuable constraints and data informing our understanding of methane emissions. A more equivalent comparison can be accomplished through long-term measurements of methane emission rates from satellite observations or possibly from continuous facility-specific ground-based measurements, and we recommend such future studies be performed.

Methane Emission Rate Comparisons between Observations and EPA GHGRP Inventory
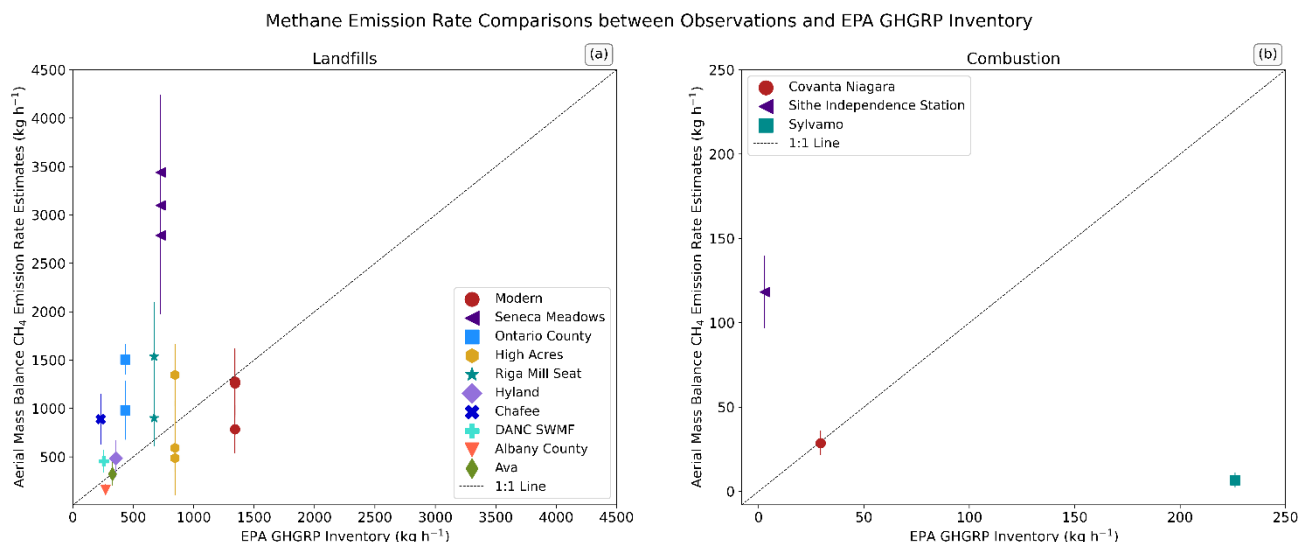
Figure 5: Comparisons between the methane emission rates estimated from this study and the 2021 EPA GHGRP Inventory at each of the landfills (a) and combustion facilities (b) visited during the study.

4 Conclusion

350   Aircraft observations were carried out for this study to estimate methane and carbon dioxide emission rates from facilities across the combustion, landfill, WWTP, and agricultural sectors. A total of 25 sites were sampled with measurements occurring in June and November/December 2021. Emission rates were calculated using a mass balance method by applying Gauss's Theorem to the observed mixing ratios and horizontal wind. Landfills were responsible for the highest estimated methane emission rates ranging from 161 kg h^{-1} at Albany County Landfill up to 3440 kg h^{-1} at Seneca Meadows Landfill. There were

355   large variations in methane emission estimates both among and within facilities between seasons. The combustion and landfill facilities had the highest CO_2 emission rates, with the Sithe Independence Station Natural Gas Power Plant significantly the highest at 300,000 kg h^{-1}. The self-reporting EPA GHGRP Inventory is, on average, generally undercounting methane emissions from landfills by a factor of 2. However, there are a few facilities where the inventory is overestimating. Out of the ten landfills sampled, five observed methane emission rates were higher than the inventory, four were within the uncertainty

360   range, and the remaining last landfill observed a lower emission rate than the inventory. These differences can be attributed to a number of factors including operational differences or seasonal influences. However, this study does not provide sufficient data and information to determine both the reason for the differences and the true emission rate. Long-term, continuous monitoring is crucial in establishing accurate and reliable emission estimates to better inform the NYS GHG Inventory and policy aimed at climate mitigation. However, the results from this study provide valuable and very much needed information

365   on methane sources and their emissions in NYS.

17

Data Availability

All data described in this manuscript can be accessed at PANGAEA under the two following DOI's for the raw data
(https://doi.org/10.1594/PANGAEA.979845) and the emission rates (https://doi.org/10.1594/PANGAEA.979843) (Catena
and Smith, 2025b, a).

Author Contribution

The study was conceptualized by JJS, LTM, EML, and MLS. Measurements were carried out by MLS. All data analysis
including scrubbing, manipulation, and facility-level emission rate calculations were done by MLS. Visualization including
maps and plots were created by AMC. The manuscript was written by AMC with contributions and feedback from all co-
authors.

Competing interests

The contact author has declared that none of the authors has any competing interests.

Disclaimer

Publisher's note: Copernicus Publications remains neutral with regard to jurisdictional claims made in the text, published
maps, institutional affiliations, or any other geographical representation in this paper. While Copernicus Publications makes
every effort to include appropriate place names, the final responsibility lies with the authors.

Acknowledgements

Financial Support

References

395 Bell, C. S., Vaughn, T. L., Zimmerle, D., Herndon, S. C., Yacovitch, T. I., Heath, G. A., Pétron, G., Edie, R., Field, R. A., Murphy, S. M., Robertson, A. M., and Soltis, J.: Comparison of methane emission estimates from multiple measurement techniques at natural gas production pads, Elementa: Science of the Anthropocene, 5, 79, https://doi.org/10.1525/elementa.266, 2017.

Bergamaschi, P., Corazza, M., Karstens, U., Athanassiadou, M., Thompson, R. L., Pison, I., Manning, A. J., Bousquet, P.,
400 Segers, A., Vermeulen, A. T., Janssens-Maenhout, G., Schmidt, M., Ramonet, M., Meinhardt, F., Aalto, T., Haszpra, L., Moncrieff, J., Popa, M. E., Lowry, D., Steinbacher, M., Jordan, A., O'Doherty, S., Piacentino, S., and Dlugokencky, E.: Top-down estimates of European CH4 and N2O emissions based on four different inverse models, Atmos Chem Phys, 15, 715–736, https://doi.org/10.5194/acp-15-715-2015, 2015.

Cambaliza, M. O. L., Shepson, P. B., Caulton, D. R., Stirm, B., Samarov, D., Gurney, K. R., Turnbull, J., Davis, K. J., Possolo,
405 A., Karion, A., Sweeney, C., Moser, B., Hendricks, A., Lauvaux, T., Mays, K., Whetstone, J., Huang, J., Razlivanov, I., Miles, N. L., and Richardson, S. J.: Assessment of uncertainties of an aircraft-based mass balance approach for quantifying urban greenhouse gas emissions, Atmos Chem Phys, 14, 9029–9050, https://doi.org/10.5194/acp-14-9029-2014, 2014.

Catena, A. M. and Smith, M. L.: Raw Aerial Observations of Methane and Carbon Dioxide at Several Sectors in New York State in 2021 [dataset]. *PANGAEA*, https://doi.org/https://doi.org/10.1594/PANGAEA.979845, 2025a.

410 Catena, A. M. and Smith, M. L.: Emission Rate Estimates of Methane and Carbon Dioxide at Several Sectors in New York State in 2021 [dataset]. *PANGAEA*, https://doi.org/https://doi.org/10.1594/PANGAEA.979843, 2025b.

CFR: eCFR :: 40 CFR Part 98 -- Mandatory Greenhouse Gas Reporting, 2009.

Conley, S., Faloona, I., Mehrotra, S., Suard, M., Lenschow, D. H., Sweeney, C., Herndon, S., Schwietzke, S., Pétron, G., Pifer, J., Kort, E. A., and Schnell, R.: Application of Gauss's theorem to quantify localized surface emissions from airborne
415 measurements of wind and trace gases, Atmos. Meas. Tech, 10, 3345–3358, https://doi.org/10.5194/amt-10-3345-2017, 2017.

Cusworth, D. H., Duren, R. M., Thorpe, A. K., Olson-Duvall, W., Heckler, J., Chapman, J. W., Eastwood, M. L., Helmlinger, M. C., Green, R. O., Asner, G. P., Dennison, P. E., and Miller, C. E.: Intermittency of Large Methane Emitters in the Permian Basin, Environ Sci Technol Lett, 8, 567–573, https://doi.org/10.1021/acs.estlett.1c00173, 2021.

Cusworth, D. H., Duren, R. M., Ayasse, A. K., Jiorle, R., Howell, K., Aubrey, A., Green, R. O., Eastwood, M. L., Chapman,
420 J. W., Thorpe, A. K., Heckler, J., Asner, G. P., Smith, M. L., Thoma, E., Krause, M. J., Heins, D., and Thorneloe, S.: Quantifying methane emissions from United States landfills, Science (1979), 383, 1499–1504, https://doi.org/10.1126/science.adi7735, 2024.

Daniels, W., Wang, J. (Lyra), Ravikumar, A., Harrison, M., Roman-White, S., George, F., and Hammerling, D.: Towards multi-scale measurement-informed methane inventories: reconciling bottom-up site-level inventories with top-down
425 measurements using continuous monitoring systems, ChemRxiv, Vancouver, 2023.

Delkash, M., Zhou, B., Han, B., Chow, F. K., Rella, C. W., and Imhoff, P. T.: Short-term landfill methane emissions dependency on wind, Waste Management, 55, 288–298, https://doi.org/10.1016/j.wasman.2016.02.009, 2016.

Delkash, M., Chow, F. K., and Imhoff, P. T.: Diurnal landfill methane flux patterns across different seasons at a landfill in Southeastern US, Waste Management, 144, 76–86, https://doi.org/10.1016/j.wasman.2022.03.004, 2022.

430   EPA: Inventory of U.S. Greenhouse Gas Emissions and Sinks: 1990-2022, 2024.

Erland, B. M., Adams, C., Darlington, A., Smith, M. L., Thorpe, A. K., Wentworth, G. R., Conley, S., Liggio, J., Li, S.-M., Miller, C. E., and Gamon, J. A.: Comparing Airborne Algorithms for Greenhouse Gas Flux Measurements over the Alberta Oil Sands, https://doi.org/10.5194/amt-2022-120, 4 May 2022.

Foster, C. S., Crosman, E. T., Holland, L., Mallia, D. V., Fasoli, B., Bares, R., Horel, J., and Lin, J. C.: Confirmation of

435   Elevated Methane Emissions in Utah's Uintah Basin With Ground-Based Observations and a High-Resolution Transport Model, Journal of Geophysical Research: Atmospheres, 122, 13,026-13,044, https://doi.org/10.1002/2017JD027480, 2017.

Guha, A., Newman, S., Fairley, D., Dinh, T. M., Duca, L., Conley, S. C., Mackenzie L. Smith, A. K. T., Duren, R. M., Daniel H. Cusworth, K. T. F., Marc L. Fischer, S. J., Yesiller, N., Hanson, J. L., and Martien, P. T.: Assessment of Regional Methane Emission Inventories through Airborne Quantification in the San Francisco Bay Area, Environ Sci Technol, 54, 9254–9264,

440   https://doi.org/10.1021/acs.est.0c01212, 2020.

IPCC: Climate Change 2007: The Physical Science Basis. Contribution of Working Group I to the Fourth Assessment Report of the Intergovernmental Panel on Climate Change, edited by: Solomon, S., Qin, D., Manning, M., Chen, Z., Marquis, M., Averyt, K. B., And, M. T., and Miller, H. L., Cambridge University Press, Cambridge, UK and New York, NY, USA, 2007.

Karion, A., Sweeney, C., Kort, E. A., Shepson, P. B., Brewer, A., Cambaliza, M., Conley, S. A., Davis, K., Deng, A., Hardesty,

445   M., Herndon, S. C., Lauvaux, T., Lavoie, T., Lyon, D., Newberger, T., Pétron, G., Rella, C., Smith, M., Wolter, S., Yacovitch, T. I., and Tans, P.: Aircraft-Based Estimate of Total Methane Emissions from the Barnett Shale Region, Environ Sci Technol, 49, 8124–8131, https://doi.org/10.1021/acs.est.5b00217, 2015.

Koene, E. F. M., Brunner, D., and Kuhlmann, G.: On the Theory of the Divergence Method for Quantifying Source Emissions From Satellite Observations, Journal of Geophysical Research: Atmospheres, 129, https://doi.org/10.1029/2023JD039904,

450   2024.

Lamb, B. K., Cambaliza, M. O. L., Davis, K. J., Edburg, S. L., Ferrara, T. W., Floerchinger, C., Heimburger, A. M. F., Herndon, S., Lauvaux, T., Lavoie, T., Lyon, D. R., Miles, N., Prasad, K. R., Richardson, S., Roscioli, J. R., Salmon, O. E., Shepson, P. B., Stirm, B. H., and Whetstone, J.: Direct and Indirect Measurements and Modeling of Methane Emissions in Indianapolis, Indiana, Environ Sci Technol, 50, 8910–8917, https://doi.org/10.1021/acs.est.6b01198, 2016.

455   Liu, Y., Paris, J.-D., Vrekoussis, M., Quéhé, P.-Y., Desservettaz, M., Kushta, J., Dubart, F., Demetriou, D., Bousquet, P., and Sciare, J.: Reconciling a national methane emission inventory with in-situ measurements, Science of The Total Environment, 901, 165896, https://doi.org/10.1016/j.scitotenv.2023.165896, 2023.

Miller, S. M. and Michalak, A. M.: Constraining sector-specific CO_2 and CH_4 emissions in the US, Atmos. Chem. Phys, 17, 3963–3985, https://doi.org/10.5194/acp-17-3963-2017, 2017.

460   Moore, D. P., Li, N. P., Wendt, L. P., Castañeda, S. R., Falinski, M. M., Zhu, J.-J., Song, C., Ren, Z. J., and Zondlo, M. A.: Underestimation of Sector-Wide Methane Emissions from United States Wastewater Treatment, Environ Sci Technol, 57, 4082–4090, https://doi.org/10.1021/acs.est.2c05373, 2023.

National Academies of Sciences, T.: Improving Characterization of Anthropogenic Methane Emissions in the United States, https://doi.org/10.17226/24987, 2018.

465   New York State Climate Action Council: New York State Climate Action Council Scoping Plan, 2022.

New York State Department of Environmental Conservation: 2020 MSW Landfill Capacity Chart, 2020.

New York State Department of Environmental Conservation: 2023 Statewide GHG Emissions Report: Summary Report, Albany, NY, USA, 2023a.

New York State Department of Environmental Conservation: 2023 Statewide GHG Emissions Report: Waste, 2023b.

470   Peischl, J., Karion, A., Sweeney, C., Kort, E. A., Smith, M. L., Brandt, A. R., Yeskoo, T., Aikin, K. C., Conley, S. A., Gvakharia, A., Trainer, M., Wolter, S., and Ryerson, T. B.: Quantifying atmospheric methane emissions from oil and natural gas production in the Bakken shale region of North Dakota, Journal of Geophysical Research: Atmospheres, 121, 6101–6111, https://doi.org/10.1002/2015JD024631, 2016.

Poulsen, T. G., Christophersen, M., Moldrup, P., and Kjeldsen, P.: Relating landfill gas emissions to atmospheric pressure
475   using numerical modelling and state-space analysis, Waste Management & Research: The Journal for a Sustainable Circular Economy, 21, 356–366, https://doi.org/10.1177/0734242X0302100408, 2003.

Rachor, I. M., Gebert, J., Gröngröft, A., and Pfeiffer, E. -M.: Variability of methane emissions from an old landfill over different time-scales, Eur J Soil Sci, 64, 16–26, https://doi.org/10.1111/ejss.12004, 2013.

Ravikumar, A. P., Li, H., Yang, S. L., and Smith, M. L.: Developing Measurement-Informed Methane Emissions Inventory
480   Estimates at Midstream Compressor Stations, ACS ES&T Air, 2, 358–367, https://doi.org/10.1021/acsestair.4c00237, 2025.

Saunois, M., Martinez, A., Poulter, B., Zhang, Z., Raymond, P. A., Regnier, P., Canadell, J. G., Jackson, R. B., Patra, P. K., Bousquet, P., Ciais, P., Dlugokencky, E. J., Lan, X., Allen, G. H., Bastviken, D., Beerling, D. J., Belikov, D. A., Blake, D. R., Castaldi, S., Crippa, M., Deemer, B. R., Dennison, F., Etiope, G., Gedney, N., Höglund-Isaksson, L., Holgerson, M. A., Hopcroft, P. O., Hugelius, G., Ito, A., Jain, A. K., Janardanan, R., Johnson, M. S., Kleinen, T., Krummel, P. B., Lauerwald,
485   R., Li, T., Liu, X., McDonald, K. C., Melton, J. R., Mühle, J., Müller, J., Murguia-Flores, F., Niwa, Y., Noce, S., Pan, S., Parker, R. J., Peng, C., Ramonet, M., Riley, W. J., Rocher-Ros, G., Rosentreter, J. A., Sasakawa, M., Segers, A., Smith, S. J., Stanley, E. H., Thanwerdas, J., Tian, H., Tsuruta, A., Tubiello, F. N., Weber, T. S., van der Werf, G. R., Worthy, D. E. J., Xi, Y., Yoshida, Y., Zhang, W., Zheng, B., Zhu, Q., Zhu, Q., and Zhuang, Q.: Global Methane Budget 2000–2020, Earth Syst Sci Data, 17, 1873–1958, https://doi.org/10.5194/essd-17-1873-2025, 2025.

490   Shindell, D., Sadavarte, P., Aben, I., Bredariol, T. de O., Dreyfus, G., Höglund-Isaksson, L., Poulter, B., Saunois, M., Schmidt, G. A., Szopa, S., Rentz, K., Parsons, L., Qu, Z., Faluvegi, G., and Maasakkers, J. D.: The Methane Imperative, Frontiers in Science, 2, https://doi.org/10.3389/fsci.2024.1349770, 2024.

Smith, M. L., Kort, E. A., Karion, A., Sweeney, C., Herndon, S. C., and Yacovitch, T. I.: Airborne Ethane Observations in the Barnett Shale: Quantification of Ethane Flux and Attribution of Methane Emissions, https://doi.org/10.1021/acs.est.5b00219, 2015.

495

United Nations Environment Programme and Climate and Clean Air Coalition: Global Methane Assessment: Benefits and Costs of Mitigating Methane Emissions, Nairobi: United Nations Environment Programme, 173 pp., 2021.

Greenhouse Gas Reporting Program (GHGRP) [FLIGHT]: https://www.epa.gov/ghgreporting/, last access: 27 June 2022.

Wecht, K. J., Jacob, D. J., Sulprizio, M. P., Santoni, G. W., Wofsy, S. C., Parker, R., Bösch, H., and Worden, J.: Spatially

500

resolving methane emissions in California: constraints from the CalNex aircraft campaign and from present (GOSAT, TES) and future (TROPOMI, geostationary) satellite observations, Atmos Chem Phys, 14, 8173–8184, https://doi.org/10.5194/acp-14-8173-2014, 2014.

Winiwarter, W. and Rypdal, K.: Assessing the uncertainty associated with national greenhouse gas emission inventories:: a case study for Austria, Atmos Environ, 35, 5425–5440, 2001.

505

Xu, L., Lin, X., Amen, J., Welding, K., and McDermitt, D.: Impact of changes in barometric pressure on landfill methane emission, Global Biogeochem Cycles, 28, 679–695, https://doi.org/10.1002/2013GB004571, 2014.

Yu, X., Millet, D. B., Wells, K. C., Henze, D. K., Cao, H., Griffis, T. J., Kort, E. A., Plant, G., Deventer, M. J., Kolka, R. K., Roman, D. T., Davis, K. J., Desai, A. R., Baier, B. C., McKain, K., Czarnetzki, A. C., and Bloom, A. A.: Aircraft-based inversions quantify the importance of wetlands and livestock for Upper Midwest methane emissions, Atmos Chem Phys, 21,

510

951–971, https://doi.org/10.5194/acp-21-951-2021, 2021.

Zhang, H., Yan, X., Cai, Z., and Zhang, Y.: Effect of rainfall on the diurnal variations of CH_4, CO_2, and N_2O fluxes from a municipal solid waste landfill, Science of The Total Environment, 442, 73–76, https://doi.org/10.1016/j.scitotenv.2012.10.041, 2013.